THE ASTRONOMICAL JOURNAL VOLUME 112, NUMBER 2 AUGUST 1996

UBVRI PHOTOMETRY OF SN 1993J IN M81: DAYS 3 TO 365

MICHAEL W. RICHMOND

Department of Astrophysical Sciences, Princeton University, Princeton, New Jersey 08544
Electronic mail: richmond@astro.princeton.edu

RICHARD R. TREFFERS, ALEXEI V. FILIPPENKO,[1] AND YOUNG PAIK

Department of Astronomy, University of California, Berkeley, California 94720-3411
Electronic mail: (treffers, alex)@astron.berkeley.edu, ypaik@bmrc.berkeley.edu

Received 1996 February 15; revised 1996 April 23

ABSTRACT

We present optical photometry of SN 1993J in M81 over the period 1993 March 30 to 1994 March 28, exactly one year after its discovery, recalibrating early data we had published in a previous paper and describing new data which cover the latter six months. At late times, the supernova's luminosity declined exponentially in *BVRI*, at a rate much faster than that of most Type II SNe. The rate of decline was smallest in *R*, probably due to the growth of strong [O I] and Hα emission lines. Measured 300 days into its evolution, SN 1993J was less luminous than other Type II SNe. © *1996 American Astronomical Society.*

1. INTRODUCTION

Supernova (SN) 1993J in M81 was discovered on 1993 March 28 UT by Francisco García. We initiated a program of follow-up photometry at Leuschner Observatory starting two days later. Results from our first season, covering days 3 to 120 after discovery, were published in Richmond *et al.* (1994; henceforth R94). We continued monitoring the SN whenever possible for the next eight months, and report here our analysis of images taken between 1993 September 26 and 1994 March 28 UT. In addition, we provide an improved set of early measurements from Leuschner Observatory, due to a recalibration of color-transformation equations; these recalibrated data replace those we listed in R94. This paper, therefore, covers the optical evolution of SN 1993J during the first 365 days after its discovery.

We describe our observations and data reduction in Sec. 2, then present the new and recalibrated light curves in Sec. 3. Section 4 contains a comparison of the late-time properties of SN 1993J to those of other SNe. We summarize our results in Sec. 5.

2. OBSERVATIONS AND DATA REDUCTION

Our procedures follow very closely those described in R94; we urge readers to consult that paper for details.

At Leuschner Observatory, we used a 50-cm and a 76-cm telescope, both reflectors equipped with CCD cameras. The full-width at half-maximum (FWHM) of stellar images was usually 3″–4″. The 50-cm telescope is equipped with an autoguider (Richmond *et al.* 1993), so we could take long exposures: 1000 to 2500 seconds. The 76-cm telescope lacks a guider, and we found that trailing occurred in any exposures longer than 300 seconds. As a result, we were unable to take images sufficiently deep to measure SN 1993J in *B* and *V* with the 76-cm telescope after 1993 November. We created bias frames by taking the median of five images each afternoon, and flatfield frames from the median of five exposures of the twilight sky; we then applied them to the raw images in the usual fashion.

As in R94, we used apertures of fixed size to extract instrumental magnitudes from each image: radius 3.″2 for the 50-cm frames, and radius 3.″4 for the 76-cm frames. We measured the sky value in a circular annulus with radii roughly 10″ and 13″.

Converting instrumental magnitudes to the standard Johnson–Cousins *UBVRI* system is somewhat problematic, since the spectrum of SN 1993J was dominated by a few very strong emission lines during our late-time observations (e.g., Filippenko *et al.* 1994). We will return to this point in Sec. 3. Observations made at Leuschner after the reduction of data in R94 suggested to us that we could improve our color corrections by using *V* and *I* as basic passbands in the photometric solution, rather than *R*. Therefore, we derived new color transformation equations for bringing raw differential photometry onto the standard system; we list these equations in the Appendix. For consistency's sake, we have re-reduced all the Leuschner Observatory data with the new color terms, and present all photometry of SN 1993J taken at Leuschner in this paper. These results should supplant those listed in R94.

The differences between measurements reduced with the old and new color terms are usually small. We compared the newly reduced measurements with those listed in R94 close to the secondary maximum, over the period $9090<\mathrm{JD}<9105$ (where JD X = Julian Date 2,440,000+X). The new *U*-, *B*-, and *V*-band measurements are roughly 0.07 mag fainter than the old ones, bringing the Leuschner *B* and *V* light curves into better agreement with those from Kitt Peak and

[1]Also associated with the Center for Particle Astrophysics, University of California at Berkeley.

 0004-6256/96/112(2)/732/10/$10.00

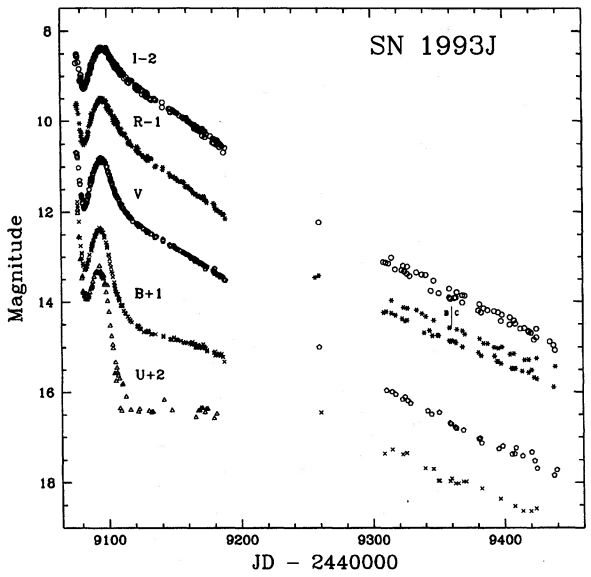

FIG. 1. *UBVRI* light curves of SN 1993J from its discovery to 1994 March 27. This figure includes data from R94 as well as new observations.

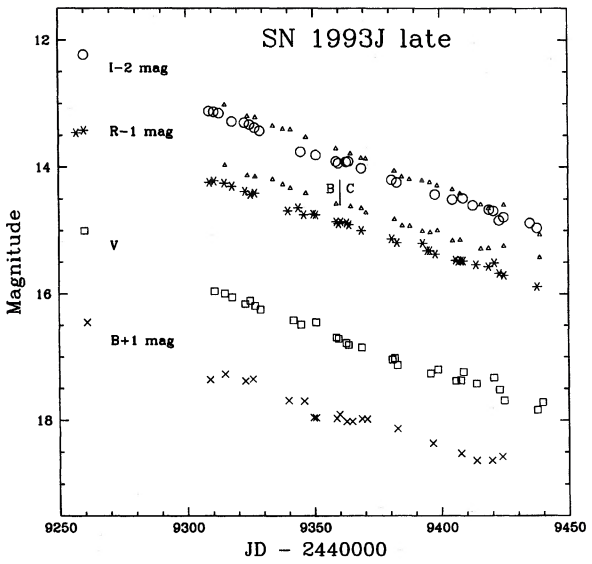

FIG. 2. Late-time light curves of SN 1993J in *BVRI*, based on observations with the Leuschner 50-cm telescope (large symbols) and the Leuschner 76-cm telescope (small triangles). The vertical bar flanked by "B" and "C" marks the time at which the comparison for *V*-, *R*-, and *I*-band observations was switched from star B to star C.

La Palma. The *R*-band data has a different correction for each of the Leuschner telescopes: the new Leuschner 50-cm data are systematically 0.06 mag fainter, and the new Leuschner 76-cm data 0.13 mag fainter, than the old ones. The new *I*-band magnitudes differ from the old by ≤ 0.02 mag in the mean.

We originally used star B (see R94) as the primary comparison for all magnitudes. However, after we increased exposure times on the 50-cm telescope on 1994 January 8 (= JD 9361), we noted that star B was saturated in the *R* and *I* images on nights of good seeing. Therefore, we switched to the fainter star C as a comparison for 50-cm *V*-, *R*-, and *I*-band data after that date, using the magnitudes listed by Lewis *et al.* (1994): $V = 14.49 \pm 0.02$, $R = 14.10 \pm 0.04$, $I = 13.79 \pm 0.05$. These are consistent with, but more precise than, the values listed in R94. We continued to use star B as the comparison in the *B*-band for 50-cm data. We mark the point at which we switched comparison stars in Figs. 1 and 2 with a vertical bar, flanked by "B" to the left (when star B was the comparison) and "C" to the right (when star C was the comparison). We detect no significant discontinuity in the light curves at this point. Note that since the 76-cm telescope has no guider, we could not increase exposure times to compensate for the fading of SN 1993J; therefore, we continued to use star B as the comparison for all 76-cm observations.

We have no measurements of the uncertainty in each individual datum. As we argue in Sec. 3, it is probably impossible to make an accurate transformation to the standard magnitude scale; Fig. 2 shows clearly that there are systematic errors in our attempts to do so. The sole simple figure of merit is the accuracy of the instrumental magnitudes. A measure of the *internal* precision of our data comes from the linear fits we make to our light curves in Sec. 3: we find that the scatter of the data around a straight line ranges from 0.04 to 0.08 mag.

3. OPTICAL LIGHT CURVES

In Fig. 1 we present our complete *UBVRI* light curves for SN 1993J, combining recalibrated data from R94 with that reported in this paper. The large gap between JD 9190 and JD 9250 represents the period when M81 was inaccessible during the night. The smaller gaps between the next few points are due to a stretch of awful weather in 1993 September and 1993 October. We show the late-time measurements alone in Fig. 2. The vertical bar at JD 9360 denotes the time at which we switched comparison stars for the 50-cm *V*-band, *R*-band, and *I*-band light curves. We list all Leuschner photometry in Tables 1 and 2.

We feel obliged to warn the reader that it is not possible to transform accurately broadband instrumental magnitudes of an object dominated by emission lines onto the standard scale. During the second half of the period covered by this paper, days 185 to 365 after discovery, SN 1993J was clearly in the "nebular phase" of evolution. Several studies (Filippenko *et al.* 1994; Finn *et al.* 1995; Barbon *et al.* 1995) of the object's spectral evolution show very strong [O I] λλ6300,6364 and [Ca II] λλ7291,7324 emission lines, as well as weaker emission from the Ca IR triplet and Mg I] λ4571. There is also a broad Hα feature underlying the [O I] line which grows relatively stronger with time. Small differences between the instrumental responses of any two telescope/filter/detector systems can lead to significant differences in the instrumental magnitudes of the same emission-line object, if a strong feature should fall at the edge of the two slightly different passbands (see Hamuy

TABLE 1. Leuschner 50-cm observations of SN 1993J.

UT Date	JD[a]	*U*	*B*	*V*	*R*	*I*	Comments
Apr 03.2	9080.7	11.43	12.02	11.67	11.36	11.08	
Apr 06.2	9083.7	11.82	12.23	11.84	11.48	11.24	
Apr 07.22	9084.72	11.84	12.16	11.73	11.37	11.16	
Apr 08.24	9085.74	11.86	12.07	11.66	11.31	11.07	
Apr 10.23	9087.73	11.67:	11.85	11.37	11.04	10.89	bad weather
Apr 11.21	9088.71	11.55	11.69	11.27	10.94	10.78	
Apr 12.2	9089.7	11.44	11.61	11.14	10.83	10.67	
Apr 13.2	9090.7	11.34	11.51	11.05	10.75	10.63	
Apr 14.2	9091.7	11.32	11.44	10.97	10.68	10.56	
Apr 16.2	9093.7	11.20	11.40	10.89	10.59	10.42	
Apr 17.2	9094.7	11.32	11.41	10.89	10.55	10.44	bad weather
Apr 18.2	9095.7	11.44	11.44	10.85	10.52	10.38	bad weather
Apr 19.2	9096.7	11.41	11.45	10.82	10.51	10.41	
Apr 20.3	9097.7	11.58	11.56	10.90	10.56	10.40	
Apr 22.2	9099.7	11.63	11.77	11.00	10.61	10.46	bad weather
Apr 23.2	9100.7	12.22	11.94	11.09	10.66	10.47	
Apr 27.2	9104.7	13.58:	12.62	11.47	10.95	10.68	
Apr 27.3	9104.8	13.58	12.62	11.47	10.95	...	
Apr 28.3	9105.7	13.75	12.75	11.59	11.06	10.76	
Apr 29.2	9106.7	13.56	12.82	11.62	11.05	10.79	
Apr 29.3	9106.8	13.57	12.83	11.63	11.06	10.80	
May 01.2	9108.7	14.35	12.93	11.74	11.16	10.86	
May 02.2	9109.7	14.41	13.08	11.83	11.23	10.92	
May 03.2	9110.7	13.82	13.08	11.89	11.27	10.97	poor seeing
May 08.2	9115.7	...	13.37	12.09	11.48	11.13	
May 09.3	9116.7	14.39	13.42	12.12	11.50	11.15	
May 14.3	9121.8	...	13.54	12.27	11.64	11.27	
May 15.3	9122.8	...	13.56	12.29	11.68	11.30	
May 16.3	9123.7	...	13.59	12.31	11.70	11.32	
May 19.3	9126.7	...	13.66	12.37	11.77	11.40	bad weather
May 21.3	9128.8	...	...	12.40	11.82	11.42	bad weather
May 22.3	9129.8	...	13.64	12.44	11.84	11.45	
May 23.3	9130.8	...	13.66	12.45	11.84	11.46	
Jun 03.3	9141.8	14.17	13.77	12.65	12.07	11.69	bad weather
Jun 09.2	9147.8	14.40	13.84	12.76	12.22	11.80	
Jun 27.2	9165.7	14.55	14.00	13.09	12.60	12.16	poor seeing
Jun 29.2	9167.7	14.41	...	13.10	...	12.19	
Jun 30.2	9168.7	14.41	13.97	...	12.64	...	
Jul 01.2	9169.7	14.35	...	13.15	...	12.22	
Jul 02.2	9170.7	14.35	14.02	...	12.67	...	
Jul 03.2	9171.7	...	...	13.13	...	12.32	poor seeing
Jul 04.2	9172.7	14.44	14.00	...	12.65	...	poor seeing
Jul 05.2	9173.7	14.37	...	13.26	...	12.35	
Jul 06.2	9174.7	14.37	14.09	...	12.79	...	poor seeing
Jul 11.2	9179.7	14.58	...	13.33	...	12.47	
Jul 12.2	9180.7	...	14.18	13.37	12.89	12.49	clouds? poor seeing
Jul 13.2	9181.7	14.48	...	...	...	...	
Jul 14.2	9182.7	...	...	13.40	...	12.52	
Jul 16.2	9184.7	...	...	13.44	...	12.57	
Jul 19.2	9187.7	...	...	13.50	...	12.69	
Sep 26.4	9256.9	...	...	...	14.46	...	
Sep 29.4	9259.9	...	...	15.00	14.42	14.23	
Sep 30.4	9260.9	...	15.45	...	...	...	
Nov 17.5	9309.0	...	16.36	...	15.24	15.12	
Nov 19.4	9310.9	...	...	15.96	15.22	15.13	
Nov 21.3	9312.8	...	...	...	...	15.15	
Nov 23.4	9314.9	...	16.27	15.99	15.25	...	
Nov 26.3	9317.8	...	...	16.05	15.30	15.28	
Dec 01.3	9322.8	...	16.38	16.16	15.38	15.30	
Dec 03.3	9324.8	...	...	16.11	15.43	15.33	
Dec 04.3	9325.8	...	16.35	...	...	...	

TABLE 1. (continued.)

UT Date	JD[a]	*U*	*B*	*V*	*R*	*I*	Comments
Dec 05.3	9326.8	...	...	16.19	15.41	15.38	
Dec 07.4	9328.9	...	...	16.25	...	15.43	
Dec 18.4	9339.9	...	16.69	...	15.69	...	
Dec 20.4	9341.9	...	...	16.42	...	...	
Dec 22.4	9343.9	...	...	...	15.64	...	
Dec 23.4	9344.9	...	...	16.49	...	15.76	
Dec 24.5	9346.0	...	16.70	...	15.75	...	
Dec 28.3	9349.8	...	16.96	...	15.74	...	
Dec 29.2	9350.7	...	16.96	16.45	15.75	15.81	
Jan 06.3, 1994	9358.8	...	16.97	16.69	15.86	15.91	
Jan 07.5	9360.0	...	16.91	16.71	15.89	15.94	
Jan 08.2	9360.7	...	...	...	15.86	...	
Jan 10.2	9362.7	...	17.02	16.78	15.88	15.92	
Jan 11.2	9363.7	...	...	16.81	15.91	15.91	
Jan 12.5	9365.0	...	17.02	...	...	...	
Jan 16.3	9368.8	...	16.98	16.85	16.00	16.02	
Jan 18.3	9370.8	...	16.98	...	...	...	
Jan 28.4	9380.9	...	...	17.04	16.13	16.20	
Jan 29.3	9381.8	...	...	17.02	...	...	
Jan 30.3	9382.8	...	17.13	17.13	16.19	16.24	
Feb 09.5	9393.0	...	...	...	16.20	...	
Feb 11.3	9394.8	...	...	...	16.32	...	
Feb 12.4	9395.9	...	...	17.26	16.32	...	
Feb 13.2	9396.7	...	17.36	...	...	...	
Feb 14.4	9397.9	...	...	...	16.37	16.43	
Feb 15.3	9398.8	...	...	17.20	...	...	
Feb 21.2	9404.7	...	...	...	...	16.51	
Feb 22.3	9405.8	...	...	17.38	16.47	...	
Feb 23.4	9406.9	...	...	...	16.49	...	
Feb 24.2	9407.7	...	17.52	17.37	16.48	...	
Feb 25.3	9408.8	...	...	17.24	16.48	16.49	
Mar 01.2	9412.7	...	...	...	...	16.60	
Mar 02.2	9413.7	...	17.63:	17.42	16.54	...	
Mar 07.2	9418.7	...	...	...	16.57	16.67	
Mar 08.3	9419.8	...	17.63:	...	...	...	
Mar 09.2	9420.7	...	...	17.33	16.51	16.69	
Mar 11.4	9422.9	...	...	17.52	16.68	16.84	
Mar 12.3	9423.8	...	17.57:	...	...	...	
Mar 13.3	9424.8	...	...	17.69	16.71	16.79	
Mar 23.4	9434.9	...	...	...	...	16.88	
Mar 26.2	9437.7	...	...	17.84	16.89	16.96	
Mar 28.3	9439.8	...	...	17.72	...	...	

[a]Julian Date −2,440,000.

et al. 1990). In addition, these spectra are very, very different from those of typical stars, which may be approximated well in the optical by a smooth continuum and weak absorption lines. Therefore, the methods one uses to transform instrumental magnitudes onto the standard system, which are based on observations of typical stars, cannot be correct when applied to SNe in the nebular phase. Figure 2 shows clearly that the measurements from the 50-cm and 76-cm Leuschner telescopes are offset from each other by ~0.30 mag in *R* and ~0.13 mag in *I*.

Nonetheless, we have used the equations listed in the Appendix to transform instrumental magnitudes into "standard" *BVRI*, for convenience in comparing the early and late photometry. We forego computing the $(B-V)$ and other colors, however, since many uses of broadband color indices are predicated on the thermal nature of their source. Trying to calculate a "temperature" from the observed colors, for example, would be a futile exercise: the SN at this stage is optically thin, and its radiation in the optical differs greatly from that of a blackbody.

As explained in Sec. 2, we re-calibrated all data collected at Leuschner Observatory, which causes small changes to the secondary peak of the light curves. We fit the light curves formed by adding the recalibrated Leuschner data to the unmodified data from Kitt Peak and La Palma, over the period JD 9085–9105, with polynomials of increasing order. We find that the fits yield identical solutions after reaching functions of the fourth and fifth order. These fits yield times of peak, and peak magnitudes; by perturbing the polynomial coefficients until the overall χ^2 value changes by unity, we

TABLE 2. Leuschner 76-cm observations of SN 1993J.

UT Date	JD[a]	U^b	B	V	R	I	Comments
Mar 30.2	9076.7	...	...	10.69:	10.65:	10.71:	bad weather
Mar 31.2	9077.7	...	10.91	10.80	10.73	10.57	bad weather
Apr 02.2	9079.7	...	11.75	11.38	11.20	11.10	bad weather
Apr 03.2	9080.7	11.16	12.02	11.68	11.44	11.06	
Apr 06.2	9083.7	...	...	11.83	11.45	11.19	
Apr 07.22	9084.72	11.86	12.16	11.75	11.41	11.13	
Apr 07.30	9084.80	11.83	12.13	11.72	11.38	11.13	
Apr 08.24	9085.74	11.86	12.07	11.63	11.26	11.05	
Apr 08.32	9085.82	11.84	12.05	11.61	11.24	11.04	
Apr 10.23	9087.73	11.82	11.82	11.31	11.02	10.86	bad weather
Apr 10.40	9087.90	11.76	11.76	11.25	11.02	10.85	bad weather
Apr 11.21	9088.71	...	...	11.23	10.90	10.75	
Apr 13.2	9090.7	11.64	11.53	11.03	10.73	10.59	
Apr 13.3	9090.8	11.65	11.54	11.04	10.74	10.59	
Apr 14.2	9091.7	...	11.41	10.96	10.64	10.52	
Apr 14.3	9091.8	11.63	11.43	10.98	10.66	10.53	
Apr 16.2	9093.7	...	11.34	10.83	10.52	10.41	
Apr 16.3	9093.8	...	11.40	10.89	10.58	10.42	
Apr 17.2	9094.7	...	...	10.82	10.50	10.38	bad weather
Apr 18.3	9095.8	...	11.44	10.85	10.56	10.38	bad weather
Apr 20.3	9097.8	...	...	10.86	10.57	10.39	
Apr 22.2	9099.7	...	...	10.99	10.70	10.37	bad weather
Apr 23.2	9100.7	12.68	11.94	11.09	10.74	10.44	
Apr 23.3	9100.8	12.69	11.95	11.10	10.75	10.47	
Apr 25.2	9102.7	...	...	11.28:	10.82	10.55:	bad weather
Apr 26.2	9103.7	...	...	...	...	10.59	
Apr 27.3	9104.8	13.30	12.56	11.47	11.00	10.68	
Apr 28.3	9105.8	13.43	12.71	11.55	10.98	10.69	
Apr 29.2	9106.7	13.51	12.83	11.62	11.05	10.75	
Apr 30.3	9107.8	13.62	12.90	11.68	11.10	10.74	
May 01.2	9108.7	13.64	12.97	11.73	11.14	10.81	
May 02.2	9109.7	13.77	13.07	11.80	11.18	10.85	
May 03.2	9110.7	13.61	13.06	11.83	11.17	10.86	poor seeing
May 04.3	9111.8	13.66:	13.20	11.92	11.28	10.92	occasional clouds
May 05.2	9112.7	13.78	13.24	11.96	11.31	10.95	
May 07.2	9114.7	13.74	13.32	12.02	11.37	11.02	
May 09.3	9116.8	13.88	13.40	12.10	11.44	11.08	
May 10.3	9117.8	13.78	13.45	12.14	11.51	11.09	
May 11.2	9118.7	...	...	12.20:	11.55:	11.10:	bad weather
May 14.3	9121.8	13.74	13.54	12.25	11.63	11.21	
May 15.3	9122.8	13.89	13.54	12.26	11.65	11.22	
May 16.3	9123.8	13.71	13.58	12.28	11.69	11.25	
May 17.3	9124.8	13.71	13.60	12.30	11.70	11.26	
May 19.3	9126.8	...	...	12.36:	11.75:	11.32:	bad weather
May 21.3	9128.8	...	13.65:	12.40	11.79	11.35	bad weather
May 22.3	9129.8	13.97:	13.66	12.45	11.85	11.36	
May 23.3	9130.8	14.01	13.66	12.43	11.86	11.40	
May 28.2	9135.7	...	13.71	12.56:	12.00	11.51	bad weather
May 29.3	9136.8	...	...	12.54:	11.98:	11.53:	bad weather
Jun 03.3	9141.8	...	13.74:	12.61	12.01	11.58:	bad weather
Jun 08.2	9146.7	14.06	13.82	12.73	12.15	11.72	
Jun 09.2	9147.7	14.21	13.81	12.75	12.21	11.76	
Jun 11.3	9149.8	14.07:	13.78	12.75	12.22	11.76	bad weather
Jun 12.2	9150.7	14.09	13.83	12.80	12.25	11.79	
Jun 13.2	9151.7	14.05	13.83	12.81	12.25	11.81	
Jun 14.3	9152.8	14.05	13.85	12.83	12.31	11.82	
Jun 16.3	9154.8	14.04	13.86	12.86	12.33	11.88	
Jun 18.3	9156.8	14.09	13.89	12.90	12.33	11.91	
Jun 19.3	9157.8	13.98	13.91	12.91	12.35	11.94	
Jun 20.3	9158.8	13.89:	13.89	12.93	12.44	11.94	poor seeing
Jun 21.2	9159.7	...	...	12.95:	12.45:	11.94:	poor seeing, clouds

TABLE 2. (continued.)

UT Date	JD[a]	U[b]	B	V	R	I	Comments
Jun 22.3	9160.8	13.83:	13.89	12.95	12.43	12.00	
Jun 23.2	9161.7	13.88	13.92	12.98	12.47:	12.00	
Jun 24.2	9162.7	14.05	13.94	13.02	12.50	12.04	light clouds?
Jun 25.2	9163.7	14.08	13.88	13.02	12.52	12.06	
Jun 26.2	9164.7	14.05	13.92	13.03	12.58	12.08	
Jun 27.2	9165.7	...	13.92	13.04	12.60	12.08	poor seeing
Jun 28.2	9166.7	14.19:	14.01	13.06	12.60	12.14	poor seeing
Jun 29.2	9167.7	14.09	13.95	13.09	12.64	12.12	
Jun 30.2	9168.7	14.19	13.99	13.11	12.65	12.17	
Jul 01.2	9169.7	14.14	14.00	13.14	12.66	12.19	
Jul 02.2	9170.7	14.33	14.00	13.14	12.68	12.20	
Jul 03.2	9171.7	...	13.93	13.17	12.69	12.20	
Jul 04.2	9172.7	...	13.98	13.17	12.72	12.23	
Jul 05.2	9173.7	14.09	14.02	13.21	12.72	12.23	
Jul 06.2	9174.7	...	14.06	13.22	12.76	12.29	
Jul 09.2	9177.7	...	...	...	...	12.33	
Jul 11.2	9179.7	...	14.12	13.30	12.81	12.39	
Jul 12.2	9180.7	...	14.10	13.26	12.84	12.40	
Jul 13.2	9181.7	...	14.16	13.36	12.96	12.42	
Jul 14.2	9182.7	...	14.16	13.39	12.95	12.42	
Jul 15.2	9183.7	...	14.14	13.40	12.98	12.48	
Jul 16.2	9184.7	...	14.19	13.41	13.01	12.49	
Jul 17.2	9185.7	...	14.15	13.43	13.01	12.52	
Jul 18.2	9186.7	...	14.21	13.44	13.06	12.55	
Jul 19.2	9187.7	...	14.32	...	13.05	...	
Jul 20.2	9188.7	...	...	13.52	13.15	12.59	
Nov 23.6	9315.1	...	...	15.99	14.97	15.02	
Dec 02.5	9324.0	...	...	...	15.13	15.20	
Dec 05.5	9327.0	...	...	...	15.15	15.22	
Dec 12.5	9334.0	...	...	...	15.19	15.35	
Dec 16.5	9338.0	...	...	...	15.27	15.40	
Dec 19.5	9341.0	...	...	...	15.33	15.41	
Dec 25.5	9347.0	...	...	...	15.41	15.53	
Jan 06.5, 1994	9359.0	...	...	...	15.58	15.71	
Jan 12.2	9364.7	...	...	...	15.62	15.79	
Jan 16.4	9368.9	...	...	...	15.65	15.86	
Jan 18.2	9370.7	...	...	...	15.72	15.87	
Jan 29.4	9381.9	...	...	...	15.82	16.06	
Feb 01.4	9384.9	...	...	...	15.92	16.15	
Feb 04.4	9387.9	...	...	...	15.93	16.19	
Feb 09.4	9392.9	...	...	...	16.01	16.21	
Feb 12.4	9395.9	...	...	...	16.03	16.24	
Feb 15.3	9398.8	...	...	...	16.00	16.29	
Feb 21.3	9404.8	...	...	...	16.16	16.35	
Feb 24.3	9407.8	...	...	...	16.15	16.42	
Mar 04.3	9415.8	...	...	...	16.29	16.59	
Mar 07.3	9418.8	...	...	...	16.28	16.65	
Mar 13.3	9424.8	...	...	...	16.25	16.60	
Mar 27.3	9438.8	...	...	...	16.43	17.07	

[a]Julian Date −2,440,000.
[b]Recall that the 76-cm U-band data does not transform well onto the standard system.

derive uncertainties in the fitted parameters. We find that all but one of the peak magnitudes listed in Table 12 of R94 are still accurate to within the stated uncertainties; the new R-band measurement lies just outside the 1σ errorbars on the old one. We list our newly derived times of maxima and peak magnitudes in Table 3. Note that the quoted uncertainties are the formal values derived from the polynomial fits, and do not include contributions from possible systematic errors in the photometric system.

TABLE 3. Fits[a] to secondary peak of light curve of SN 1993J.

Passband	Date of peak[b]	Observed mag
U	9092.86±0.13	11.31±0.04
B	9093.47±0.08	11.38±0.01
V	9094.88±0.08	10.85±0.01
R	9095.35±0.06	10.53±0.02
I	9096.30±0.05	10.37±0.02

[a]Includes Julian Dates 2,449,085–2,449,105.
[b]Julian Date −2,440,000.

TABLE 4. Slope of linear fit to late-time[a] light curves, mag/100 days.

Telescope	*B*	*V*	*R*	*I*
50-cm	1.22±0.08	1.41±0.07	1.27±0.04	1.42±0.04
76-cm	...	...	1.21±0.04	1.53±0.04

[a]Fit includes points with Julian Dates 2,449,300–2,449,440.

As Fig. 2 shows, the late-time light curves are remarkably linear in a graph of magnitude versus time. In each passband, the few points around JD 9260 fall slightly above the line extrapolated backward from the later data. It seems likely, therefore, that the light curve may not have reached a strictly linear decline until some time in 1993 October, around 200 days after discovery.

The *B*-band light curve stops dropping after JD 9410, but we suspect that this is a spurious feature. The 50-cm telescope was reaching its detection limits in these last observations of SN 1993J, which began to merge with the background light of M81. It is our experience that when an object falls to the detection limit, aperture photometry usually yields an incorrectly bright measurement. In our analysis of SN 1993J, we centered our aperture on the highest apparent signal near the position of the SN, rather than on a position fixed relative to other field stars; thus, we must have been biased toward including local peaks in the statistical noise. Barbon *et al.* (1995), who used a larger telescope and more sophisticated methods of measurement, list consistently fainter *B* magnitudes from JD 9368 onward, and the difference grows larger after JD 9410. We therefore place a ":" in Tables 1 and 2 to denote these measurements as uncertain. The differences between our measurements and those of Barbon *et al.* in *VRI* are small enough that one may ascribe them to differences in transformations to the standard system.

The *V*, *R*, and *I* data all show a remarkably linear decline in magnitudes per day, corresponding to an exponential decrease in flux with time. We list the slope γ of each curve, in units of magnitudes per 100 days, over the period JD 9300–9440 (days 225–365 after discovery) in Table 4. The slopes we determine are slightly less steep than those tabulated by Barbon *et al.* (1995) because they include somewhat earlier data in their calculations.

As Fig. 1 shows, SN 1993J faded very quickly after reaching the "knee" in its *B* or *V* light curve, falling with $\gamma \approx 2.0$ in *VRI* from days 43 to 120 after discovery. At later times, however, the decline slowed to $\gamma = 1.2-1.4$. The isotope ^{56}Co is thought to produce the main energy input into the SN during this time period. With a half-life of 77.3 days, ^{56}Co would yield a decline of $\gamma = 0.98$. At no time after the secondary maximum do we observe SN 1993J to fade this slowly.

We followed the practice of R94 by summing the optical fluxes and correcting for several possible amounts of extinction.[2] However, since we increased the exposure times substantially near the end of our observations, we were generally unable to acquire images in all four passbands (*BVRI*) on a single night. Therefore, we merged together data from two consecutive nights to form the last five tabulated *BVRI* sums. Converting this summed flux into pseudo-magnitude units yields an overall optical decline rate closest to that of the *R* band. The *R*-band contributes roughly 40% of the *BVRI* flux at late times, no doubt due to the very strong [O I] and Hα emission lines. Tables 5 and 6 contain the re-calibrated fluxes at earlier times and Table 7 contains the summed optical fluxes for SN 1993J at late times. We list the observed fluxes together with those which have been corrected for two values of extinction. Figure 3 displays the observed optical flux on a logarithmic scale.

TABLE 5. Summed optical fluxes[a] of SN 1993J: Leuschner 50-cm *UBVRI*.

JD[b]	Observed	E(*B*−*V*)=0.08	E(*B*−*V*)=0.40
9080.75	3.938e-10	5.053e-10	1.457e-09
9083.73	3.262e-10	4.162e-10	1.171e-09
9084.74	3.497e-10	4.450e-10	1.239e-09
9085.73	3.706e-10	4.709e-10	1.302e-09
9087.73	4.604e-10	5.847e-10	1.611e-09
9088.69	5.181e-10	6.586e-10	1.820e-09
9089.73	5.667e-10	7.201e-10	1.988e-09
9090.72	6.118e-10	7.784e-10	2.158e-09
9091.72	6.498e-10	8.261e-10	2.282e-09
9093.72	7.044e-10	8.946e-10	2.464e-09
9094.71	6.981e-10	8.846e-10	2.412e-09
9095.73	7.019e-10	8.864e-10	2.380e-09
9096.70	7.050e-10	8.908e-10	2.397e-09
9097.70	6.598e-10	8.309e-10	2.205e-09
9099.71	6.039e-10	7.589e-10	1.998e-09
9100.70	5.410e-10	6.740e-10	1.706e-09
9104.68	3.723e-10	4.572e-10	1.082e-09
9105.70	3.366e-10	4.130e-10	9.732e-10
9106.70	3.291e-10	4.038e-10	9.529e-10
9108.70	2.979e-10	3.643e-10	8.457e-10
9109.71	2.761e-10	3.373e-10	7.785e-10
9110.74	2.676e-10	3.278e-10	7.682e-10
9116.71	2.160e-10	2.637e-10	6.076e-10
9141.79	1.364e-10	1.676e-10	3.993e-10
9147.78	1.218e-10	1.496e-10	3.564e-10
9165.71	9.071e-11	1.120e-10	2.724e-10

[a]In units of erg cm^{-2} s^{-1}. Uses Bessell 1979 flux calibration.
[b]Julian Date − 2,440,000.

4. DISCUSSION

Comparing the decline rates of SN 1993J with those of other SNe in the interval 200–400 days after explosion, we find in Table 8 that it is far from a "normal" Type II. In fact, the Type II-L SN 1990K (Cappellaro *et al.* 1994) is the only other Type II, to our knowledge, which declined as rapidly as SN 1993J. On the other hand, Turatto *et al.* (1990) list decline rates of $\gamma \approx 1.5$ in *B* and *V* for a set of five Type I

[2]We discovered an error in the program we used to calculate the summed optical fluxes in R94; specifically, we overestimated the extinction corrections for the E(*B*−*V*)=0.32 case in Tables 14 and 15, and in Fig. 11. One can make the tables and figure correct by replacing the label E(*B*−*V*)=0.32 with E(*B*−*V*)=0.40. This problem was corrected before we calculated fluxes for this paper. We choose E(*B*−*V*)=0.40 as our representative of the large-extinction case in this paper (see Tables 5, 6, and 7) so that the reader may directly combine La Palma and Kitt Peak data from Table 14 in R94 with that from the tables in this paper.

TABLE 6. Summed optical fluxes[a] of SN 1993J: Leuschner 76-cm *BVRI*.

JD[b]	Observed	E($B-V$)=0.08	E($B-V$)=0.40
9150.75	1.153e-10	1.407e-10	3.225e-10
9151.74	1.145e-10	1.398e-10	3.207e-10
9152.78	1.113e-10	1.358e-10	3.118e-10
9154.77	1.081e-10	1.320e-10	3.040e-10
9156.75	1.060e-10	1.294e-10	2.976e-10
9157.77	1.040e-10	1.270e-10	2.923e-10
9158.76	1.009e-10	1.234e-10	2.851e-10
9160.77	9.933e-11	1.215e-10	2.817e-10
9161.74	9.705e-11	1.187e-10	2.747e-10
9162.75	9.414e-11	1.151e-10	2.669e-10
9163.72	9.401e-11	1.151e-10	2.687e-10
9164.74	9.103e-11	1.115e-10	2.601e-10
9165.74	9.030e-11	1.106e-10	2.582e-10
9166.75	8.728e-11	1.068e-10	2.484e-10
9167.74	8.702e-11	1.066e-10	2.490e-10
9168.74	8.496e-11	1.041e-10	2.429e-10
9169.74	8.344e-11	1.022e-10	2.389e-10
9170.73	8.273e-11	1.014e-10	2.372e-10
9171.73	8.263e-11	1.014e-10	2.390e-10
9172.72	8.079e-11	9.910e-11	2.329e-10
9173.73	7.976e-11	9.775e-11	2.288e-10
9174.72	7.693e-11	9.433e-11	2.212e-10
9179.71	7.203e-11	8.837e-11	2.076e-10
9180.72	7.202e-11	8.843e-11	2.085e-10
9181.70	6.707e-11	8.232e-11	1.939e-10
9182.70	6.688e-11	8.207e-11	1.932e-10
9183.70	6.544e-11	8.043e-11	1.906e-10
9184.70	6.397e-11	7.858e-11	1.857e-10
9185.70	6.375e-11	7.840e-11	1.862e-10
9186.70	6.153e-11	7.564e-11	1.794e-10

[a]In units of erg cm^{-2} s^{-1}. Uses Bessell 1979 flux calibration.
[b]Julian Date −2,440,000.

SNe; the single Type Ib event in their sample with data in V had $\gamma=1.1$. Barbon *et al.* (1995) indicate that the Type Ib SN 1990I had a much larger rate of decline. Recent near-UV photometry of the Type Ia SN 1992A by Ruiz-Lapuente *et al.* (1995) shows decline rates of $\gamma=1.3-1.4$ mag per day

TABLE 7. Summed optical fluxes[a] of SN 1993J: Leuschner 50-cm *BVRI*.

JD[b]	Observed	E($B-V$)=0.08	E($B-V$)=0.40	comments
9260.00	1.619e-11	2.005e-11	4.891e-11	merged nights
9322.80	6.382e-12	7.914e-12	1.947e-11	
9325.00	6.247e-12	7.764e-12	1.926e-11	merged nights
9345.00	4.553e-12	5.660e-12	1.406e-11	merged nights
9350.70	4.269e-12	5.281e-12	1.283e-11	
9358.80	3.869e-12	4.795e-12	1.175e-11	
9360.00	3.854e-12	4.787e-12	1.183e-11	
9362.70	3.738e-12	4.628e-12	1.130e-11	
9368.80	3.521e-12	4.375e-12	1.084e-11	
9382.80	2.934e-12	3.650e-12	9.092e-12	
9398.5	2.488e-12	3.093e-12	7.669e-12	merged nights
9408.5	2.243e-12	2.782e-12	6.849e-12	merged nights
9413.5	2.059e-12	2.553e-12	6.268e-12	merged nights
9420.5	2.079e-12	2.580e-12	6.354e-12	merged nights
9423.5	1.840e-12	2.294e-12	5.771e-12	merged nights

[a]In units of erg cm^{-2} s^{-1}. Uses Bessell 1979 flux calibration.
[b]Julian Date −2,440,000. In cases where data from several nights have been merged, the date is a rough average.

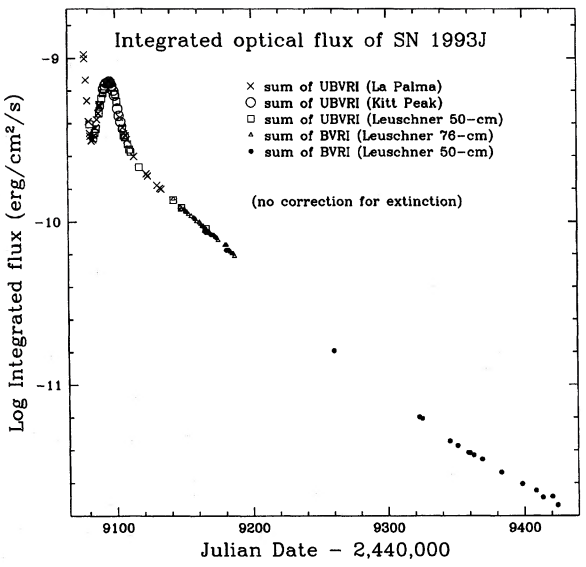

FIG. 3. Summed optical fluxes of SN 1993J from its discovery to 1994 March 11. No correction for interstellar extinction has been made.

between 77 and 291 days after maximum light. Overall, SN 1993J appears as an intermediate between Types I and II; we agree with Barbon *et al.* that its late-time light curves compare most favorably with those of Type Ia. As Barbon *et al.* state, it is likely that the steep decline of SN 1993J is due to the relatively small mass of its ejecta blanket. Most models of the explosion yield ejecta ranging from $1.8M_\odot$ (Wheeler *et al.* 1993) to $4.6M_\odot$ (Woosley *et al.* 1993); only Höflich *et al.* (1993) advocate as much as $\sim 10M_\odot$, which might be typical of a classical Type II-P event. It would be especially interesting to compare the late-time evolution of SN 1993J with that of additional Type Ib events, since many groups have commented on the similarity between SN 1993J and SNe Ib [see Wheeler & Filippenko (1996) for a review].

At later times, we agree with Filippenko *et al.* (1994) and Patat *et al.* (1994) that the interaction of the ejecta with the circumstellar wind of the progenitor may provide an important energy source. Patat *et al.* measure a flux in the Hα emission line which decreases in proportion to t^{-3}, consistent with a simple ejecta-wind explanation. However, since the broadband R flux declines exponentially with time, rather than as t^{-3}, it appears that the Hα line does not dominate the total R-band flux we measured.

Patat *et al.* (1994) also note that many Type II SNe have similar luminosities during their late-time exponential decline, which they characterize by M_V^{300}, the absolute V magnitude 300 days after explosion. They find that a sample of eight events has a mean absolute magnitude $\langle M_V^{300}\rangle = -12.6\pm0.5$, with the assumption that $H_0=75$ km s^{-1} Mpc^{-1}. If we use the Cepheid distance $\mu=27.8$ to M81 (Freedman *et al.* 1993), and note that at 300 days after the explosion, SN 1993J had apparent magnitude $m_V\approx16.9$, we derive $M_V^{300}\approx-10.9-A_V$. In R94, we found evidence that the extinction to SN 1993J fell in the range $A_V=0.25$ to 1.00 mag. Thus, we conclude that SN 1993J had $M_V^{300}\approx-11.2$ to -11.9, perhaps a little fainter than the av-

TABLE 8. Comparison of late-time decline rates for SNe, mag/100 days.

SN Type	*B*	*V*	*R*	Source
Ia + Ib	1.51±0.04 (n=1)	1.46±0.24 (n=4)	···	Turatto *et al.* 1990
II	0.74±0.11 (n=8)	0.89±0.04 (n=6)	0.99±0.01 (n=2)	Turatto *et al.* 1990
II	···	0.96±0.12 (n=8)	···	Patat *et al.* 1994
SN 1993J	1.22±0.08	1.41±0.07	1.24±0.04	this paper

erage Type II at 300 days. However, since the distances adopted by Patat *et al.* are based on redshifts to the host galaxies, in contrast to that of M81 [whose radial velocity is negative, $v_{21} = -34$ km s^{-1} (de Vaucouleurs *et al.* 1991)], it is not easy to compare SN 1993J with more distant SNe in a consistent manner.

If we restrict the comparison to SNe whose distances have been measured by the Expanding Photosphere Method (EPM), we can make a more consistent comparison. In Table 9, we list four Type II SNe from the list of Patat *et al.* (1994) for which Schmidt *et al.* (1994) measured distances via EPM. Using the apparent magnitudes and extinctions listed in Patat *et al.*, and the EPM distances, we calculate absolute magnitudes M_V^{300} for each event. Each SN appears slightly more luminous in this table than in Patat *et al.* There have been several applications of EPM to determine the distance of SN 1993J, although it is clear that the method may yield questionable results, due to the lack of a large hydrogen envelope (Schmidt *et al.* 1993) and the uncertain extinction (Prabhu *et al.* 1995). As Table 9 shows, the use of EPM distances implies that SN 1993J was much less luminous than other Type II SNe at an age of 300 days.

5. CONCLUSIONS

We present *BVRI* photometry of SN 1993J from days 185 to 365 after discovery, extending our earlier coverage of its evolution. We also give recalibrated results from the first 6 months after explosion. The optical light curves show a linear decline after day 200, fading at $\gamma \approx 1.2-1.4$ mag per 100 days. This is much quicker than the great majority of Type II SNe, and closer to the steep declines of Type I events. We ascribe the steep decline of SN 1993J to a small ejecta blanket. On its exponential tail, 300 days after explosion, there is evidence that SN 1993J may have been less luminous than most Type II SNe.

M. W. R. thanks the Department of Astrophysical Sciences at Princeton University. We are grateful to Sun Microsystems, Inc. (Academic Equipment Grant Program) and to Photometrics, Ltd. for equipment donations that were vital to the acquisition and reduction of data at Leuschner Observatory. Financial support for this research was provided to A. V. F. and his group at UC Berkeley through NSF Grant Nos. AST-8957063, AST-9115174, and AST-9417213.

APPENDIX: PHOTOMETRIC SOLUTIONS FOR LEUSCHNER

The following solutions are identical to those in Richmond *et al.* (1996), but include an additional set of equations for the 76-cm telescope based on $(r-i)$ color. We present all the solutions for clarity.

For the Leuschner 50-cm telescope, we observed the M67 "dipper" asterism (see Schild 1983) on 1993 April 1, 1993 April 6, 1994 January 7, 1994 October 8, and 1994 October 29, to determine the first-order color terms which transform instrumental magnitudes to the standard Johnson–Cousins system. The terms C_V, C_{BV}, etc., are the differences between the zero-points of the instrumental and standard magnitudes, which vary from night to night. Since we always measured the brightness of SN 1993J relative to that of some other star in the same image, these terms were not involved in the photometric solutions, and were set to zero in our calculations. We include second-order color-dependent extinction corrections *only* for instrumental B-band measurements, as described in the Appendix to R94; we denote the extinction-corrected B-band instrumental values by b^0 in the equations below. For the Leuschner 50-cm telescope, we find

$$V = v + 0.02(v-i) + C_V,$$

$$(B-V) = 1.15(b^0-v) + C_{BV},$$

$$(U-B) = 1.20(u-b^0) + C_{UB},$$

TABLE 9. Comparison of M_V^{300} for Type II SNe with EPM distances.

SN	m_V^{300}[a]	$(m-M)$[b]	A_V[c]	M_V^{300}	Source
SN 1969L	17.15	30.13	0.18	−13.16	
SN 1979C	18.71	30.88	0.45	−12.62	
SN 1980K	18.04	28.78	1.20	−11.94	
SN 1988A	18.60	31.51	0.00	−12.91	
SN 1993J	16.9	28.0	0.31	−11.4	Schmidt *et al.* 1993
SN 1993J	16.9	26.7	0.25	−10.1	Prabhu *et al.* 1995, upper limit
SN 1993J	16.9	28.5	0.99	−12.6	Prabhu *et al.* 1995, lower limit
SN 1993J	16.9	28.0	0.31	−11.4	Baron *et al.* 1995

[a]From Patat *et al.* 1994, except SN 1993J (this paper).
[b]From Schmidt *et al.* 1994, except SN 1993J (see source).
[c]From Patat *et al.* 1994, except SN 1993J (see source).

$$(V-R)=0.87(v-r)+C_{VR},$$

$$I=i+0.05(v-i)+C_I.$$

We used images of M67 taken on 1994 October 31, 1994 November 8, 1994 November 11, and 1994 November 13 to calculate the color terms for the Leuschner 76-cm telescope, finding

$$V=v+0.01(v-i)+C_V,$$

$$(B-V)=1.16(b^0-v)+C_{BV},$$

$$(U-B)=1.86(u-b^0)+C_{UB},$$

$$(V-R)=0.88(v-r)+C_{VR},$$

$$I=i+0.02(v-i)+C_I.$$

At late times, when we were unable to acquire V-band images of SN 1993J with the 76-cm telescope, we employed color terms based on $(r-i)$;

$$R=r+0.21(r-i)+C_R,$$

$$I=i+0.04(r-i)+C_I.$$

REFERENCES

Barbon, R., Benetti, S., Cappellaro, E., Patat, F., Turatto, M., & Iijima, T. 1995, A&AS, 110, 513

Baron, E., *et al.* 1995, ApJ, 441, 170

Cappellaro, E., Danziger, I. J, Della Valle, M., Gouiffes, C., & Turatto, M. 1995, A&A, 293, 723

de Vaucouleurs, G., de Vaucouleurs, A., Corwin, Jr., H. G., Buta, R. J., Paturel, G., & Fouqué, P. 1991, Third Reference Catalog of Bright Galaxies (Springer, New York)

Filippenko, A. V., Matheson, T., & Barth, A. J. 1994, AJ, 108, 2220

Finn, R. A., Fesen, R. A., Darling, G. W., Thorstensen, J. R., & Worthey, G. S. 1995, AJ, 110, 300

Freedman, W. L., *et al.* 1993, ApJ, 427, 628

Hamuy, M., Suntzeff, N. B., Bravo, J., & Phillips, M. M. 1990, PASP, 102, 888

Höflich, P., Langer, N., & Duschinger, M. 1993, A&A, 275, L29

Lewis, J. R., *et al.* 1994, MNRAS, 266, L27

Patat, F., Barbon, R., Cappellaro, E., & Turatto, M. 1994, A&A, 282, 731

Prabhu, T. P., *et al.* 1995, A&A, 295, 403

Richmond, M. W., Treffers, R. R., & Filippenko, A. V. 1993, PASP, 105, 1164

Richmond, M. W., Treffers, R. R., Filippenko, A. V., Paik, Y., Leibundgut, B., Schulman, E., & Cox, C. V. 1994, AJ, 107, 1022

Richmond, M. W., *et al.* 1996, 111, 327

Ruiz-Lapuente, P., Kirshner, R. P., Phillips, M. M., Challis, P. M., Schmidt, B. P., Filippenko, A. V., & Wheeler, J. C. 1995, ApJ, 439, 60

Schild, R. E. 1983, PASP, 95, 1021

Schmidt, B. P., *et al.* 1993, Nature, 364, 600

Schmidt, B. P., Kirshner, R. P., Eastman, R. G., Phillips, M. M., Suntzeff, N. B., Hamuy, M., Maza, J., & Avilés, R. 1994, ApJ, 432, 42

Turatto, M., Cappellaro, E., Barbon, R., Della Valle, M., Ortolani, S., & Rosino, L. 1990, AJ, 100, 771

Wheeler, J. C., *et al.* 1993, ApJ, 417, L71

Wheeler, J. C., & Filippenko, A. V. 1996, in Supernovae and Supernova Remnants, edited by R. McCray and Z. W. Li (Cambridge University Press, Cambridge) (in press)

Woosley, S. E., Eastman, R. G., Weaver, T. A., & Pinto, P. A. 1994, ApJ, 429, 300